Nucleic Acids Research, 2006, Vol. 34, No. 12 ***3577–3584***
doi:10.1093/nar/gkl482

H1 RNA polymerase III promoter-driven expression of an RNA aptamer leads to high-level inhibition of intracellular protein activity

Jing Mi[1], Xiuwu Zhang[2], Zahid N Rabbani[3], Yingmiao Liu[1], Zhen Su[1], Zeljko Vujaskovic[3], Christopher D. Kontos[4], Bruce A. Sullenger[1] and Bryan M. Clary[1,*]

[1]Department of Surgery, [2]Department of Psychiatry, [3]Department of Radiation Oncology and [4]Department of Medicine, Duke University Medical Center, Durham, NC, USA

Received May 8, 2006; Revised June 22, 2006; Accepted June 24, 2006

ABSTRACT

Aptamers offer advantages over other oligonucleotide-based approaches that artificially interfere with target gene function due to their ability to bind protein products of these genes with high affinity and specificity. However, RNA aptamers are limited in their ability to target intracellular proteins since even nuclease-resistant aptamers do not efficiently enter the intracellular compartments. Moreover, attempts at expressing RNA aptamers within mammalian cells through vector-based approaches have been hampered by the presence of additional flanking sequences in expressed RNA aptamers, which may alter their functional conformation. In this report, we successfully expressed a 'pure' RNA aptamer specific for NF-κB p50 protein (A-p50) utilizing an adenoviral vector employing the H1 RNA polymerase III promoter. Binding of the expressed aptamer to its target and subsequent inhibition of NF-κB mediated intracellular events were demonstrated in human lung adenocarcinoma cells (A549), murine mammary carcinoma cells (4T1) as well as a human tumor xenograft model. This success highlights the promise of RNA aptamers to effectively target intracellular proteins for *in vitro* discovery and *in vivo* applications.

INTRODUCTION

Over the last 20 years, different strategies have been developed to manipulate gene expression and/or function with oligonucleotides. These include antisense oligonucleotides, ribozymes and, more recently, small interfering RNA (1). Although these approaches in principle allow the rational design of regulatory sequences, they are poorly adapted to target proteins (2,3). The idea of using single-stranded nucleic acids (DNA and RNA aptamers) to target protein molecules is based on the ability of short sequences (20mers to 80mers) to fold into unique 3D conformations that enable them to bind targeted proteins with high affinity and specificity (4–6). RNA aptamers have been expressed successfully inside eukaryotic cells, such as yeast and multicellular organisms, and have been shown to have inhibitory effects on their targeted proteins in the cellular environment (7–9). However, simple and reliable methods for expressing RNA aptamer that target intracellular proteins in mammalian cells are currently lacking. Attempts at expressing RNA aptamers through vector-based approaches have been hampered by the presence of flanking sequences in expressed RNA aptamers which can inhibit their ability to fold into functional conformations, thus rendering the aptamer inert (10–12). Therefore, it will be critical to develop vectors that will allow expression of 'pure' RNA aptamer sequences following delivery into targeted cells. Although there are potential gene therapy implications of such an expression system, the greater benefits would be realized in exploring the biology of intracellular protein pathways and in identifying and confirming the relevancy of candidate proteins for targeted therapeutics.

Constitutively high levels of nuclear NF-κB activity have been described in many types of cancer cells and abrogation of constitutive NF-κB activity results in apoptosis of treated tumor cells (13,14). A 31 nt RNA aptamer was shown previously to target the p50 subunit of NF-κB in yeast (15,16). However, effects of the RNA aptamer on NF-κB transcriptional activity in mammalian cells have not yet been demonstrated. In this study, we successfully produced an adenoviral vector to express the 'pure' RNA aptamer of NF-κB p50 protein (termed A-p50). The expressed A-p50 effectively inhibits NF-κB transactivation and induces apoptosis in

*To whom correspondence should be addressed at Box 3629 and Box 2633, Duke University Medical Center, Durham, NC 27710, USA. Tel: +1 919 684 3381; Fax: +1 919 668 0487; Email: clary001@mc.duke.edu

The authors wish it to be known that, in their opinion, the first two authors should be regarded as joint First Authors

both human lung adenocarcinoma cells (A549) and murine mammary carcinoma cells (4T1) and also delays tumor growth in a human tumor xenograft model.

MATERIALS AND METHODS

Cell culture

The following cell lines were used in this study: (i) HEK 293, an adenovirus E1 gene-transduced human embryonic kidney cell line for adenovirus packaging and expansion; (ii) A549, a human lung adenocarcinoma cell line obtained from American Type Culture Collection (Manassas, Virginia); and (iii) 4T1 mouse mammary carcinoma cells were obtained from Dr Fred Miller's laboratory (Michigan Cancer Foundation, Detroit, MI). These cell lines were grown in DMEM (Invitrogen Inc., Carlsbad, CA) with 10% fetal bovine serum, 100 U/ml penicillin and 100 μg/ml streptomycin at 37°C in 5% CO_2.

A-p50 RNA aptamer expression cassette design

A 31 nt A-p50 minigene sequence (ATCTTGAAACTGTT-TTAAGGTTGGCCGATC) was synthesized for transcription of A-p50 aptamer. Two complementary oligonucleotides were synthesized and annealed to yield the 31 nt A-p50 expression minigene. A tract of six thymidines was included at the 3′ end to terminate RNA pol III transcription. BamHI- and HindIII-compatible overhangs were introduced at each end to facilitate ligation into the pSilencer-3.0 vector. An H1 promoter is upstream of the BamHI site to initiate transcription precisely at the +1 position. The resultant plasmid is the pSilencer-A-p50 (Figure 1A). As a negative control, a 47 nt small sequence (TTCTCCGAACGTGTCACG-TTTCAAGAGAACGTGACACGTTCGGAGAA) with no known target (siNT) in the human genome was cloned into the adenoviral vector in place of the A-p50 minigene (17,18).

Plasmid construction and adenovirus production

The AdEasy system (Stratagene, La Jolla, CA) was used to generate recombinant adenoviruses Ad-A-p50 and Ad-siNT. The A-p50-encoding gene expression cassette (eA-p50), including the H1 promoter, the A-p50 minigene sequence and six terminal thymidines, was excised by EcoRI/HindIII from pSilencer-A-p50 and subcloned into the EcoRV/HindIII sites of pAdTrack after blunting the EcoRI site (Figure 1B). The resultant plasmid, pAdTrack-A-p50, was packaged into recombinant adenovirus, according to the manufacturer's protocol. Briefly, the pAdtrack-A-p50 plasmid was linearized with PmeI and recombined with pAdeasy-1 plasmid in *rec*A+ BJ5183 *Escherichia coli*. The recombined pAdeasy-A-p50 plasmid was linearized with PacI and then transfected into the 293 cells to obtain recombinant adenovirus, Ad-A-p50. Large-scale virus preparation was performed according to established protocols. The control virus, Ad-siNT, was produced in a similar manner. Both viruses express enhanced green fluorescent protein (EGFP) under the direction of a CMV promoter, which allows assessment of viral infection.

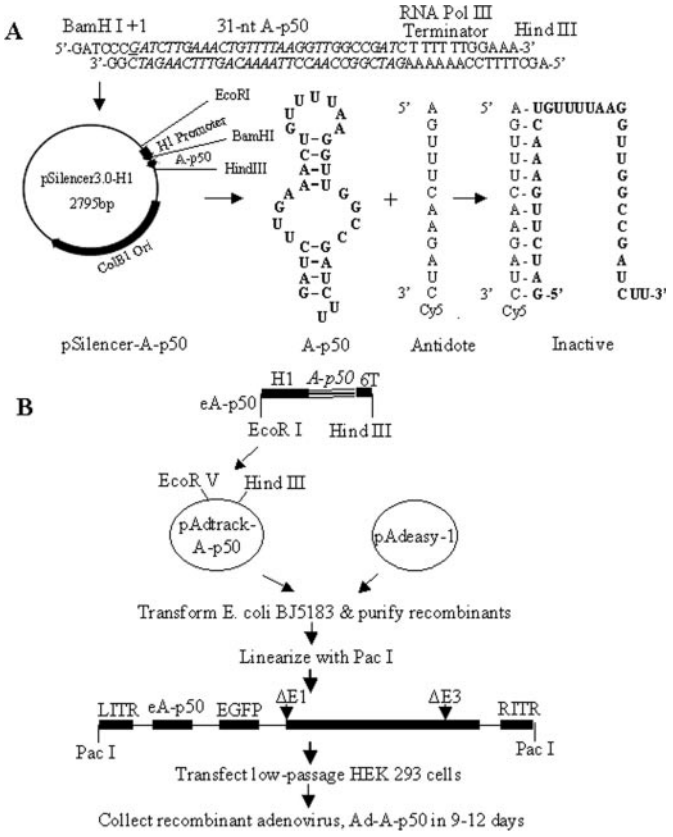

Figure 1. Strategy for production of A-p50 aptamer expression vectors. (**A**) Construction of A-p50 aptamer expression cassette. Two complementary oligonucleotides containing the 31 nt A-p50 minigene (italic) and six thymidines to terminate transcription were ligated into the expression vector pSilencer-3.0 downstream of a human H1 gene-based RNA polymerase III promoter. Upon transcription, two additional uridines are present at the A-p50 3′ end. The predicted secondary structure suggests that these uridines have a negligible effect on the A-p50 conformation. A 12 nt antidote complementary to a portion of the A-p50 RNA aptamer sequence was designed and predicted to inactivate A-p50 by blocking its secondary structure formation. (**B**) Production of A-p50 expressing adenovirus. The expression cassette, eA-p50, was excised from pSilencer-A-p50 and inserted into the pAdTrack vector to produce pAdTrack-A-p50. After recombination with the virus backbone, pAdEasy-1, in *rec*A+ BJ5183 *E.coli*, the recombinant adenoviral vector was linearized with PacI and transfected into HEK293 cells to allow large-scale virus production.

Northern blot analysis

Total RNA was extracted from Ad-siNT- or Ad-A-p50-infected A549 cells (10 MOI, 24 h). Total RNA (10 μg) was loaded onto a 2% denaturing formaldehyde gel and transferred to a nylon membrane. Prehybridization and hybridization were performed with the ExpressHyb buffer (Invitrogen) at 68°C. The membrane was rinsed per the manufacturer's instructions (Invitrogen) and exposed to film for signal detection. For A-p50 RNA detection, the antisense oligonucleotide of A-p50 (5′-GATCGGCCAACCTTAAAACAGTTTCAAG-ATC-3′) was ^{32}P-labeled by using [γ-^{32}P]ATP and T4 polynucleotide kinase. The ^{32}P-end labeled oligonucleotide probe was used directly for hybridization.

Cell homogenization, nuclear fractionation and western blot analysis

A549 cells were infected with Ad-A-p50 or Ad-siNT (10 MOI, 24 h). Nuclear extracts were obtained by incubating cells with hypotonic buffer A [20 mM HEPES, pH 7.0, 10 mM KCl, 1 mM $MgCl_2$, 10% glycerol, 0.5 mM DTT and 0.25 mM phenylmethylsulfonyl fluoride (PMSF)] for 10 min on ice. The lysates were centrifuged at 200 *g* for 10 min and the pellet was then washed three times with buffer A. To extract nuclear proteins for western blot analysis, 50 µl buffer A containing 300 mM NaCl and 0.1% NP-40 was finally applied to the pellet. For total cell protein extraction, cells were homogenized in protein inhibitor containing buffer (5 mM Tris–HCl, pH 7.4 and 2 mM EDTA) and sonicated for 10–15 s. After centrifuge to remove large cell debris, supernatants were harvested and concentrations were determined by the *DC* protein assay (Bio-Rad Laboratories Inc., Hercules, CA). Proteins were electrophoresed on a 4–15% SDS–PAGE gel and then transferred to a nitrocellulose membrane. After blocking, the membrane was incubated with the primary antibody for 2 h, washed with phosphate-buffered saline (PBS)/0.1% Tween-20 three times and then incubated with horseradish peroxidase-conjugated secondary antibody (IgG). After washing, the signal was visualized by use of the ECL kit (Amersham, Arlington Heights, IL). The primary antibody to Bcl-XL was purchased from BD Science (Palo Alto, CA), to NF-κB p50 was from Upstate (Lake Placid, NY), and to cleaved caspase-3 was from Cell Signaling Technology (Beverly, MA).

Intracellular binding assay

Dishes (10 cm) of Ad-A-p50- or Ad-siNT-infected A549 cells (5 MOI for 24 h) were treated with 1% formaldehyde for 10 min at 37°C to crosslink oligonucleotides and associated proteins. Cells were then homogenized by incubating cells with 200 µl lysis buffer (20 mM HEPES, 100 mM NaCl, 1.5 mM $MgCl_2$, 0.5% NP-40, 10 µg/ml aprotinin, 0.5 mM PMSF and 10% v/v RNase inhibitor) for 30 min, followed by brief sonication on ice. Co-immunoprecipitation (IP) of A-p50 RNA with NF-κB p50 was performed by incubating 100 µl of protein extracts with 5 µg rabbit anti-NF-κB (p50) antibody or non-specific rabbit IgG as a negative control overnight at 4°C. Protein A–agarose slurry (Upstate, Waltham, MA) was added for 2 h at 4°C. The beads were spun at 3000 *g* for 4 min at 4°C and the pellet was washed three times with 1 ml ice-cold lysis buffer. The final pellet was resuspended in 500 µl of solution D (20 mM HEPES, 20% glycerol, 0.1 M KCl, 0.2 mM EDTA and 0.5 mM DTT) and incubated with proteinase K (40 µg/ml) for 1 h at 42°C. Protein-associated RNA was isolated by phenol-chloroform extraction and isopropanol precipitation and reverse-transcribed with an A-p50 reverse primer, A-p50R (5′-*GTCCTAAGGTAGCAG*AGATCGGCCAACCT-3′). The presence of A-p50 RNA was verified by PCR with an A-p50 forward primer, A-p50F (5′-*GGATAACAGGGTAAT*-GATCTTGAAACTGTT-3′) together with A-p50R. Because the 31 nt A-p50 is so small and is difficult to visualize on a gel, these primers were designed to contain 15 additional bases (italics), which do not match any known mammalian gene sequences. A two-step PCR was performed (94°C, 30 s; 50°C, 40 s) for 30 cycles to amplify a 62 bp A-p50 band. PCR products were verified by sequencing.

NF-κB-driven GFP reporter assay

In order to assay the function of NF-κB, the NF-κB *cis*-reporting plasmid (pNF-κB-hrGFP) with a humanized green fluorescent protein (hrGFP) reporter was utilized (Stratagene). In this system, hrGFP gene is driven by a synthetic promoter containing NF-κB binding site repeats. A549 cells (1×10^6) were co-transfected with a total of 4 µg DNA, consisting of 1 µg pNF-κB-hrGFP and 3 µg of either pSilencer 3.0 empty plasmid or pSilencer-A-p50. pSilencer 3.0 vector alone was used as a negative control for hrGFP expression. The electro-transfection approach was performed according to the manufacturer's recommendations (Bio-Rad, Philadelphia, PA). To ensure equal transfection efficacy, the transfection procedure was strictly controlled. After a 36 h incubation, hrGFP expression was visualized by fluorescence microscopy.

Cell analysis by flow cytometry

GFP detection by flow cytometry has been described in detail previously (19). A549 cells (1×10^6) were electro-transfected as described above. The transfected cells were allowed to recover and express hrGFP for 36 h, then cells were pelleted, washed and fixed with PBS-1% formaldehyde. A sample of 5×10^5 cells was analyzed using a BD Bioscience FACS Calibur. Data were analyzed and presented using Cell Quest Software. The percentage of hrGFP-expressing cells was calculated by dividing the number of green-fluorescent cells observed by the total number of cells counted.

MTT assay

The MTT assay (Sigma, St Louis, MO) examines the activity of metabolic enzymes in the mitochondria of live cells. Cells were grown to 70% confluence in 96-well plates and infected with Ad-A-p50 or Ad-siNT (MOI of 10) for 24 h. The MTT assay was carried out by an established protocol (18). The values were normalized against non-infected cells and results were analyzed using Student's *t*-test.

Hoechst 33342 staining for apoptotic morphology

Cells were grown to 70% confluence in 12-well plates, infected with Ad-A-p50 or Ad-siNT (10 MOI) for 24 h, and then the cells were fixed in methanol:acetic acid (3:1) for 5 min at 4°C and washed three times with water. Subsequently, the cells were stained with Hoechst 33342 (5 µg/ml; Calbiochem, La Jolla, CA) for 10 min at room temperature. The cells were then washed three times with water, and apoptotic nuclei were visualized by fluorescence microscopy.

Protection analysis by antidotes

A 12 nt antidote complementary to a portion of the A-p50 RNA aptamer was designed (5′-mAmGmUmUmUmCm-AmAmGmAmUmC-Cy5-3′). All of the 12 nt were methylated to protect the antidote from RNase degradation. The 3′-terminal Cy-5 modification allows assessment of transfection efficacy. As a negative control (siNT), we adapted the no-target sequence used for Ad-siNT in the same manner with methyl and Cy-5 modifications

(5′-mTmTmCmTmCmCmGmAmAmCmGmTmGmTmCm-AmCmGmT-Cy5-3′). A549 cells were grown to 30–40% confluence in 12-well plates, infected with Ad-siNT or Ad-A-p50 (10 MOI) for 1 h, then transfected with antidote (150 pmol) or siNT control RNA (120 pmol) by using lipofectamine-based approach and continually cultured for 23 h. Under fluorescence microscopy, the efficacy of antidote and control siNT transfection was shown by Cy-5 (red) visualization, and the efficacy of Ad-siNT and Ad-A-p50 infection was shown by GFP expression (green). The apoptotic cell nuclei were visualized by Hoechst 33342 (blue) staining. Quantitative analysis of the extent of apoptosis in different cell populations was conducted in 12 random fields of 3 independent wells with the same treatment. Student's *t*-test was used to assess significance.

Tumor growth delay studies

For *in vivo* analysis of tumor growth, 1×10^6 A549 tumor cells in 50 µl of PBS were injected subcutaneously into the flanks of Balb/C nude mice. When tumors grew to sizes of 4–5 mm in diameter, adenoviruses (1×10^8 plaque-forming units in 25 µl) were injected into the tumors (day1 in Figure 4A). Adenoviruses were injected every 48 h for 2 weeks, and tumor growth was measured every 48 h. Growth curves were plotted as the mean of tumor volume relative to that on the first day of injection ± SEM. Each treatment group consisted of six to seven animals. The following formula was used to calculate tumor volume: $V = (1/2)W^2 \times L$ (W, the shortest dimension and L, the longest dimension) (18). The results were analyzed by one-way repeated-measures ANOVA and the interactive term was evaluated by Bonferroni corrected pair-wise comparisons.

Immunohistochemistry

Immunohistochemistry was performed using 10–12 µm serial sections of frozen tissue. Sections were fixed in ice-cold acetone for 10 min. After endogenous peroxidase activity was quenched with 3% hydrogen peroxide for 15 min, tumor sections were blocked with 10% donkey serum for 15 min. Sections were incubated in anti-rabbit primary antibodies against Bcl-XL (1:800; BD-Pharmingen, USA), activated caspase-3 (1:100; Cell Signaling Technology) and Ki67 (1:2000; Vector-Labs, USA) for 1 h at room temperature, respectively. After washing in PBS, biotinylated donkey anti-rabbit antibody (Jackson Immunoresearch, PA) was applied for 30 min at room temperature, followed by application of an avidin–biotin complex (Vectastain ABC kit; Vector Labs, Inc., Burlingame). Staining was visualized with the Nova Red kit (Vector Labs, Inc.), and slides were counterstained with hematoxylin. Omission of the primary antibody served as negative control. Staining was evaluated at lower (×100) and higher (×400) magnifications of four to five randomly chosen fields.

RESULTS AND DISCUSSION

In an attempt to achieve high level of expression of RNA aptamers that maintain their affinity for the targeted protein, we adopted the pSilencer-3.0 vector (Ambion Inc., Austin, TX) that employs H1 RNA polymerase III promoter for high level of small RNA expression (20). The advantage of this vector is that RNA transcription starts accurately at the initial base of inserted sequences and terminates with the addition of two uridines (U) at the 3′ end. Based on RNA structure predictions, the additional uridines should have minimal effect on aptamer folding (Figure 1A). This approach also avoids non-specific effects that might be caused by transcription of additional regions of vector sequence. To our knowledge, this approach has not been used previously to express RNA aptamers intracellularly.

We generated a recombinant adenovirus, Ad-A-p50 (Figure 1B) to deliver our aptamer, A-p50 consisting of 31 nt of optimized sequence (16). A potential advantage of aptamers as therapeutic tools, which was demonstrated recently by Rusconi *et al*. (21), is that complementary sequences can be designed and used as 'antidotes', which will bind and neutralize the aptamers activity. As such, we designed a 12 nt antidote of A-p50 aptamer that is predicted to inhibit A-p50 ability to fold into its functional conformation (Figure 1A). As a negative control, we replaced the 31 nt A-p50 sequence with a non-targeting small interfering RNA (Ambion Inc.) to produce Ad-siNT. This small RNA is predicted to fold into a hairpin loop, but importantly it has been shown previously to exhibit no biological effects on cell viability (17,18).

To determine whether the resulting adenoviral vector Ad-A-p50 could express the A-p50 RNA aptamer, total RNA from Ad-A-p50- or Ad-siNT-infected human lung adenocarcinoma A549 cells was subjected to northern blot analysis. A low molecular weight band (~33 nt) corresponding to the size of the A-p50 RNA aptamer (plus two end uridines) was detected only in RNA from Ad-A-p50-infected cells, indicating that this adenovirus expressed the inserted sequence (Figure 2A). An additional high molecular weight band was also detected, which corresponded to the size of viral genome DNA that was not effectively excluded in our RNA isolation process. These data demonstrate that the modified adenovirus used here can serve as an efficient vector to transduce RNA aptamers.

To verify the binding between A-p50 and NF-κB, RT–PCR was used to amplify the A-p50 aptamer present in NF-κB immunoprecipitates from infected A549 cells, which was then visualized by agarose gel electrophoresis (Figure 2B). A band consistent with A-p50 was amplified only when cell lysates were immunoprecipitated with anti-NF-κB and not with a non-specific rabbit IgG. This band was sequenced and verified to contain the amplified A-p50 sequence. Consistent with the previous reports (13,14,22), nuclear NF-κB p50 expression was readily detectable in A549 cells (Figure 2C and D). Interestingly, infection of A549 cells with Ad-A-p50 virus resulted in an ~2.6-fold reduction in nuclear localized p50 (Figure 2C), but had no effect on total cellular NF-κB p50 expression (Figure 2D). NF-κB exists in the cytoplasm in an inactive state, where it is bound to the inhibitor protein IκB, which inhibits NF-κB translocation to the cell nucleus. Upon activation, NF-κB translocates to the nucleus where it influences gene transcription (23). However, IκBα expressed in the nuclear compartment abrogates NF-κB/DNA interactions and promotes the export of NF-κB back to the cytoplasm (24). Thus, we speculated that the Ad-A-p50-induced reduction

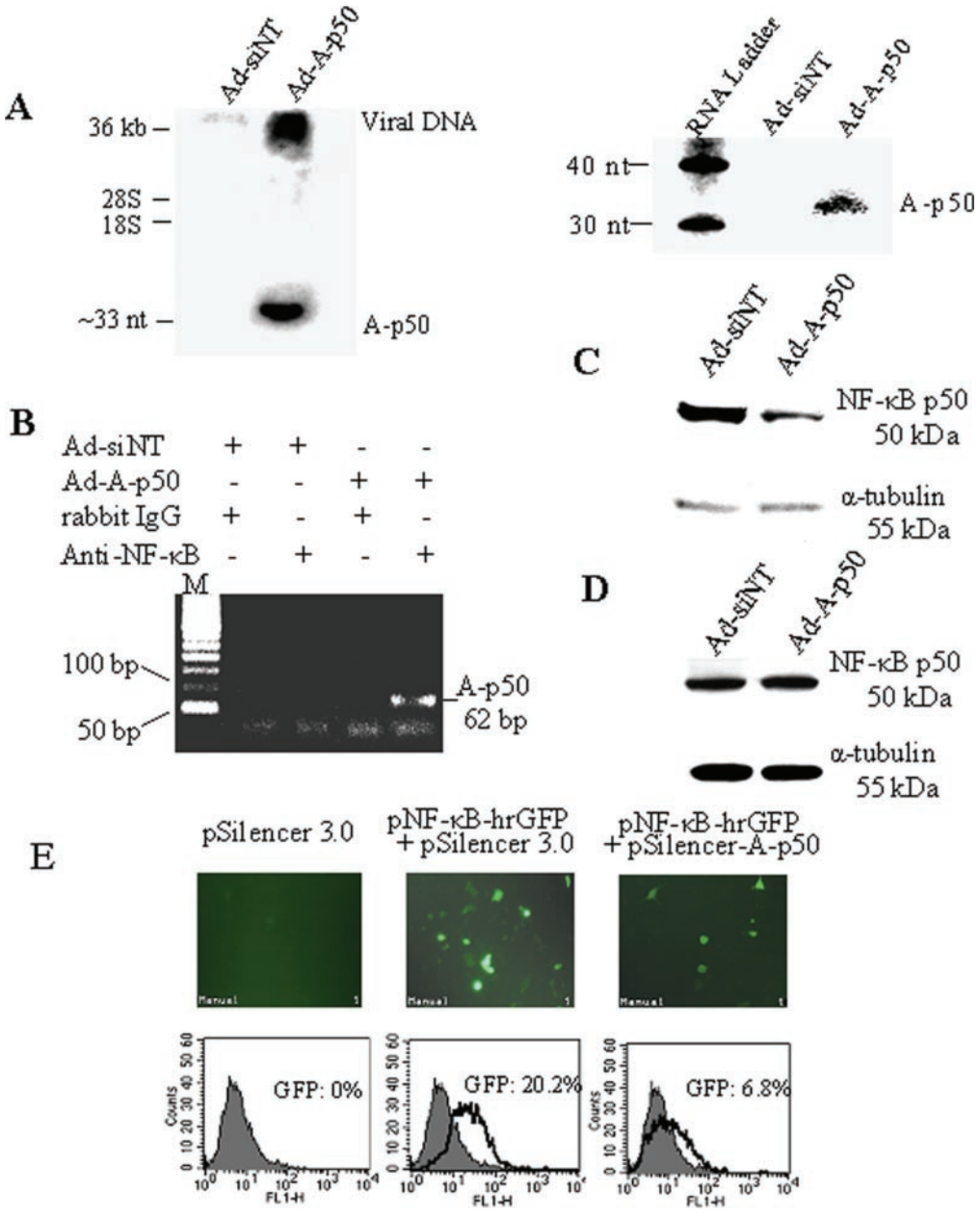

Figure 2. Expressed A-p50 exhibits biological activity in A549 cells. (**A**) Northern blot analysis of A-p50 expression. An expressed A-p50 band (lower panel) and a viral genomic DNA band (upper panel) are visualized only in Ad-A-p50-infected A549 cells (Ad-A-p50). The size of the lower band was determined by acrylamide gel electrophoresis relative to a 10 nt RNA ladder (Ambion). (**B**) Intracellular binding of A-p50 to NF-κB p50 protein. RT–PCR confirms the presence of A-p50 aptamer in anti-NF-κB p50 immunoprecipitates from Ad-A-p50-infected A549 cells. M, 50 bp DNA ladder. (**C**) Western blot analysis of NF-κB p50 protein in nuclear fractions. Ad-A-p50-infected A549 cells show a decrease in nuclear NF-κB p50 expression (Ad-A-p50) compared with Ad-siNT-infected A549 cells. Expression of α-tubulin was used as a protein loading control. (**D**) Western blot analysis of NF-κB p50 protein in whole cell lysates. Ad-A-p50-infected A549 cells show no changes in total NF-κB p50 protein level compared to Ad-siNT-infected A549 cells. (**E**) Inhibition of NF-κB-mediated transcriptional activity by A-p50 in cells. Upper panel: By fluorescence microscopy, the pNF-κB-hrGFP-transfected A549 cells show high GFP protein expression (middle panel) compared to none in the empty plasmid-transfected cells (left panel). Co-transfection of A-p50 expression plasmid and pNF-κB-hrGFP results in a decrease in hrGFP expression (right panel). Lower panel: quantitative analysis of GFP expression by flow cytometry. Co-transfection of A-p50 expression vector with pNF-κB-hrGFP results in about a 70% decrease in GFP expression (right panel) compared to co-transfection of pSilencer3.0 and pNF-κB-hrGFP (middle panel). As a control, transfection of empty plasmid alone showed no GFP expression (left panel).

in nuclear NF-κB expression was due to A-p50 ability to block NF-κB binding to DNA, resulting in increase of IκBα-mediated export to the cytoplasm. These data demonstrate that A-p50 interacts specifically with p50 protein in mammalian cells following adenoviral delivery and expression.

We next used a NF-κB reporter system (Stratagene) to examine whether interaction with A-p50 affects NF-κB's transcriptional activity. Upon binding NF-κB, GFP expression is induced and can be visualized by fluorescence microscopy. Because Ad-A-p50 also expresses GFP, we tested effects of A-p50 on NF-κB-mediated transcription following

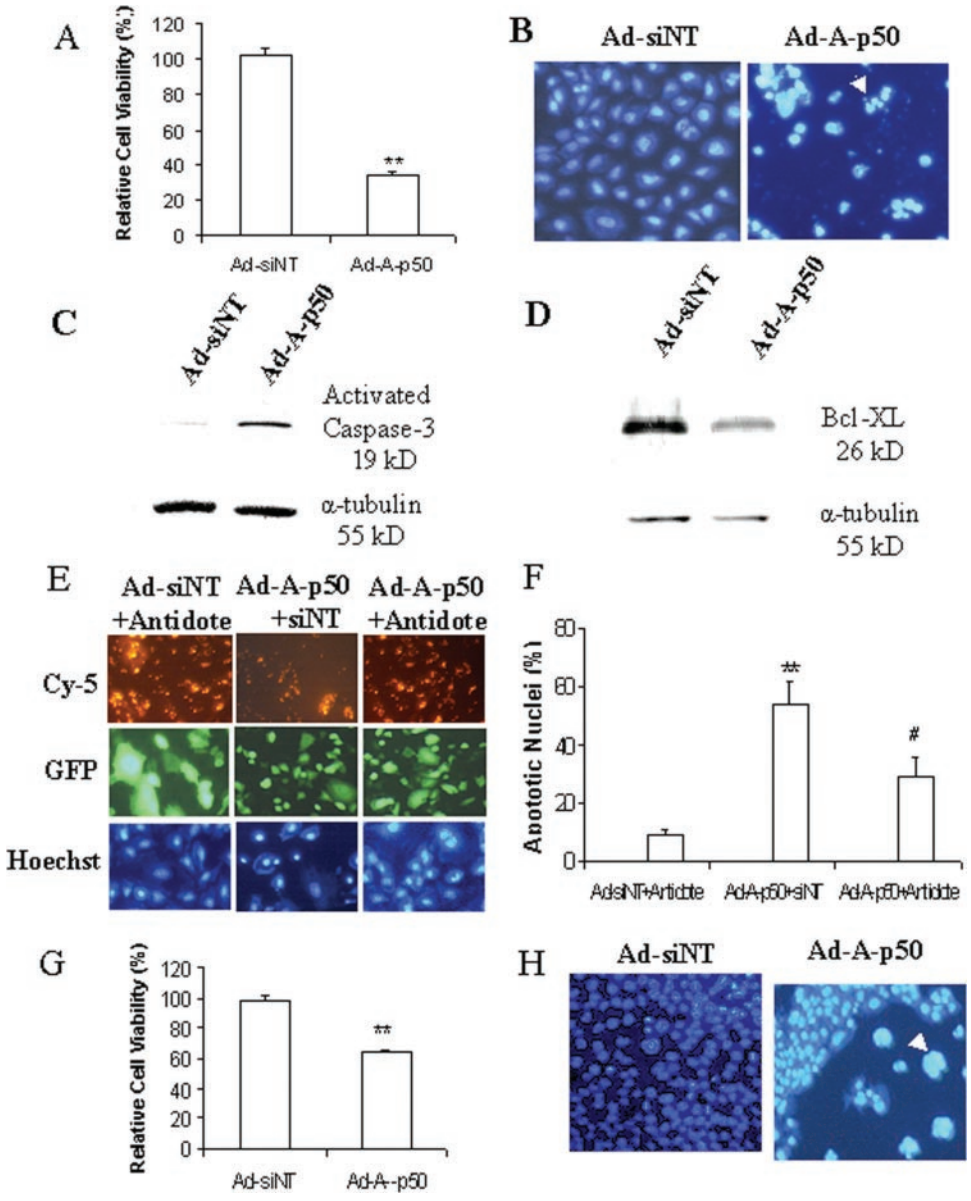

Figure 3. A-p50 affects tumor cell survival *in vitro* through inhibition of NF-κB-mediated transcriptional activation. (**A**) MTT assay of cell viability. Ad-A-p50-infected A549 cells show a significant decrease in cell viability (Ad-A-p50) compared to Ad-siNT-infected cells, $n = 3$–5 per group, $^{**}P = 0.0001$. (**B**) Hoechst 33342 staining of apoptotic nuclei. Ad-A-p50-infected A549 cells (Ad-A-p50) show increased numbers of apoptotic nuclei compared with Ad-siNT-infected cells. (**C**) Western blot analysis of cleaved, active caspase-3. Ad-A-p50 infection increases activated caspase-3 levels in A549 cells. (**D**) Western blot analysis of Bcl-XL expression. Ad-A-p50 infection results in downregulation of Bcl-XL expression. (**E**) Analysis of antidote-mediated protection in A549 cells. Upper panel shows the transfection efficacy of antidote and control siNT small RNA (Cy-5). Middle panel shows the infection efficiency of Ad-siNT and Ad-A-p50 (GFP). Lower panel shows Hoechst 33342 staining of apoptotic nuclei. The increased apoptotic nuclei in Ad-A-p50-infected A549 cells (Ad-A-p50) were partly reversed by the antidote. (**F**) Quantification of apoptosis in (E). Bars, mean ± SD of data from 12 fields in 3 independent wells with the same treatment. $^{**}P = 0.0004$ versus Ad-siNT + antidote control group; $^{*}P = 0.042$ versus Ad-A-p50 + siNT group. (**G**) MTT assay of cell viability. Ad-A-p50-infected 4T1 cells show a significant decrease in cell viability (Ad-A-p50), $n = 3$–5 per group, $^{**}P = 0.0001$. (**H**) Hoechst 33342 staining of apoptotic nuclei. Ad-A-p50-infected 4T1 cells (Ad-A-p50) show increased numbers of apoptotic nuclei compared to Ad-siNT-infected cells.

plasmid transfection with pSilencer-A-p50. Transfection of a plasmid encoding the NF-κB-hrGFP reporter into A549 cells resulted in readily detectable GFP expression as a result of endogenous NF-κB activity. Notably, co-transfection of pSilencer-A-p50 along with the NF-κB-hrGFP reporter plasmid resulted in marked attenuation of GFP expression (Figure 2E, upper panels). Using quantitative flow cytometry, co-transfection of pSilencer-A-p50 induced an ~70% inhibition in NF-κB-mediated GFP expression (Figure 2E, lower panels). These data clearly illustrate that A-p50 aptamer expression in cells abolishes binding of NF-κB to its target DNA and inhibits NF-κB-mediated gene transcription.

Several studies have shown that activated NF-κB promotes cell survival while suppression of NF-κB activity abrogates this process (25). To investigate whether inhibition of NF-κB DNA-binding activity could result in cell death *in vitro*, the MTT assay, Hoechst 33342 staining of apoptotic nuclei and western blotting of cleaved caspase-3 were used to

evaluate cell viability and apoptosis. MTT assay showed a significant decrease in cell viability in Ad-A-p50-infected A549 cells (65.3%) compared with Ad-siNT controls ($P < 0.001$) (Figure 3A). Hoechst 33342 staining demonstrated that the number of nuclei with apoptotic morphological features was increased in Ad-A-p50-infected A549 cells (Figure 3B). Consistent with this observation, western blotting demonstrated an increase in cleaved caspase-3 in Ad-A-p50-infected A549 cells (Figure 3C). These data demonstrate that intracellular delivery of A-p50 induces apoptosis. The constitutively high level of nuclear NF-κB activity in A549 cells has been shown to induce upregulation of anti-apoptotic genes, such as Bcl-XL (22). Thus, if the expressed A-p50 aptamer has biological activity in A549 cells, Bcl-XL expression should be diminished by Ad-A-p50 infection. Indeed, western blotting showed that the Bcl-XL level was reduced in Ad-A-p50-infected A549 cells (Figure 3D).

To verify that apoptosis of Ad-A-p50-infected A549 cells was a specific effect of the expressed A-p50 aptamer, we investigated whether a complementary antidote sequence could inhibit this effect. Transfection of the antidote resulted in a partial but significant reversal of Ad-A-p50 apoptotic effect, as demonstrated by changes in nuclear morphology (Figure 3E and F). To explore whether the expressed A-p50 aptamer exhibits biological activity in other cell types, we evaluated apoptosis in Ad-A-p50-infected 4T1 mouse mammary carcinoma cells. The MTT assay and Hoechst nuclear staining showed decreased cell viability (Figure 3G) and increased apoptotic nuclei (Figure 3H) in Ad-A-p50-infected 4T1 cells. Taken together, these *in vitro* data demonstrate that the expressed A-p50 RNA aptamer specifically induces apoptosis in cultured tumor cell lines by binding NF-κB p50 and reversing NF-κB-mediated expression of genes like Bcl-XL.

Although one of the benefits to the expression of RNA aptamers is in exploring biological pathways such as in the development and testing of targeted therapeutics, the major contribution of aptamer lies in the realm of gene therapeutics. As such, we next determined whether local instillation of Ad-A-p50 could impair the growth of established tumors. NF-κB is necessary for tumor cell proliferation, invasion and angiogenesis (25,26); therefore, inhibitors of NF-κB should abrogate tumor growth. To examine the effects of Ad-A-p50 on tumor growth inhibition, A549 tumors were established in nude mice. Intra-tumoral injection of Ad-A-p50 resulted in significant tumor growth inhibition compared with Ad-siNT ($P < 0.05$) beginning 2 weeks after the first virus injection (day 1) (Figure 4A). To investigate the mechanisms of Ad-A-p50 effects on tumors *in vivo*, we performed immunohistochemistry to analyze markers of proliferation and apoptosis. Expression of the cell proliferation marker Ki67 and the cell survival protein Bcl-XL were greatly reduced in Ad-A-p50-injected tumor tissues compared with Ad-siNT-infected tumors, while expression of cleaved (active) caspase-3 was dramatically increased (Figure 4B). These findings demonstrate that tumor growth inhibition *in vivo* by Ad-A-p50 is due, at least in part, to loss of proliferative capacity and enhanced apoptosis.

To date, expression of RNA aptamers for *in vivo* applications has met with limited success, in part due to interference from flanking vector sequences. Martell *et al*. (10) developed

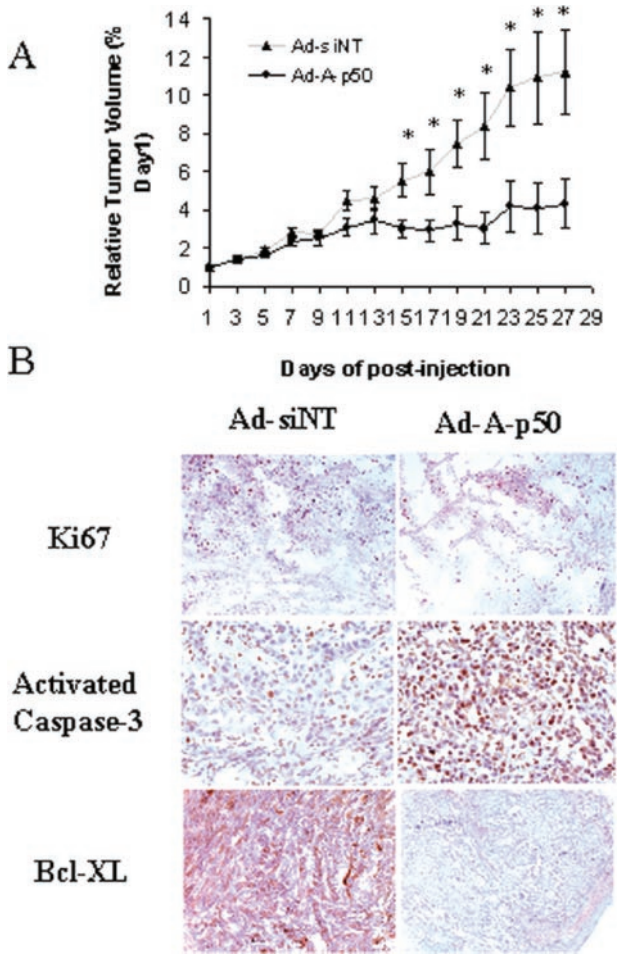

Figure 4. A-p50 affects A549 cell survival *in vivo* through inhibition of NF-κB-mediated transcriptional activation. (**A**) Tumor growth delay. Growth curves are plotted as the mean of tumor volume normalized to tumor size at the time of infection ± SEM. $n = 6–7$ animals per group. A significant difference in tumor volume was observed beginning 2 weeks after the first virus injection (day 1), which persisted for the remainder of the study, $^*P < 0.05$. (**B**) Immunohistochemical analysis of Ki67, activated caspase-3, and Bcl-XL protein expression. Ad-A-p50 virus-injected tumor tissues show a decrease in Ki67 protein expression compared with Ad-siNT-injected tumor tissues (×100 magnification, brownish red nuclear stain), consistent with a decrease in cell proliferation. Ad-A-p50 virus-injected tumor tissues show a marked increase in activated caspase-3 levels (×400 magnification, brownish red nuclear stain) as well as an obvious decrease in Bcl-XL expression (×100 magnification, brownish red stain) compared with Ad-siNT-injected tumor tissues, consistent with enhanced tumor cell apoptosis.

an expression cassette SELEX strategy to randomize flanking sequences and select for chimeric tRNAs that retained high affinity for E2F. Despite the apparent success of this approach, repeated SELEX is technically complex, tedious and might not be universally effective. Blind *et al*. (12) developed a vaccinia virus-based RNA expression system based on double infection with two recombinant vaccinia viruses encoding T7 polymerase and aptamer, respectively, to achieve high-level cytoplasmic expression of RNA aptamers directed against the intracellular domain of the β_2 integrin LFA-1. However, this approach utilized a vector with 5′ and 3′ flanking stem–loop structures as RNA-stabilizing motifs, which were also required for correct termination of the T7 transcripts. It is not clear whether these flanking

stem–loop structures would be a universally effective strategy for other aptamers. Furthermore, vaccinia virus is less well established as a gene delivery vector for *in vivo* applications, and the immunogenicity of T7 polymerase will likely limit its therapeutic utility. An ideal approach to *in vivo* aptamer delivery would provide efficient delivery to the target cells while effecting high-level expression of 'pure' aptamer. Indeed, the RNA aptamer expression vector presented in this study meets these requirements, and we believe it will provide a more reliable approach to the delivery of RNA aptamers for *in vitro* investigations and *in vivo* therapy.

One potential limitation to the approach described here is that transcription by the H1 promoter cannot be precisely controlled. Recently, two different groups have described successful regulation of transcription by integrating the bacterial tetracycline operon sequence (tetO) into the U6 promoter (27,28), which offers the potential to optimize our system.

In conclusion, expression of RNA aptamers whose binding ability and biological activity are retained is feasible utilizing the expression system described in this study. As very specific inhibitors of known proteins can be readily created through aptamer approaches, this expression system may be valuable in selective inhibition of intracellular proteins for *in vi*vo application.

ACKNOWLEDGEMENTS

We thank Chuan-Yuan Li for assistance with animal experiments. We thank Mark Dewhirst and Yiting Cao for assistance with fluorescence imaging. Funding to pay the Open Access publication charges for this article was provided by Department of Surgery, General Research Hepatobiliary Fund.

Conflict of interest statement. None declared.

REFERENCES

1. Randall,G., Grakoui,A. and Rice,C.M. (2003) Clearance of replicating hepatitis C virus replicon RNAs in cell culture by small interfering RNAs. *Proc. Natl Acad. Sci. USA*, **100**, 235–240.
2. Toulme,J.J., Di Primo,C. and Moreau,S. (2001) Modulation of RNA function by oligonucleotides recognizing RNA structure. *Prog. Nucleic Acid Res. Mol. Biol*., **69**, 1–46.
3. Toulme,J.J., Darfeuille,F., Kolb,G., Chabas,S. and Staedel,C. (2003) Modulating viral gene expression by aptamers to RNA structures. *Biol. Cell*, **95**, 229–238.
4. Ellington,A.D. and Szostak,J.W. (1990) *In vitro* selection of RNA molecules that bind specific ligands. *Nature*, **346**, 818–822.
5. Ellington,A.D. and Szostak,J.W. (1992) Selection *in vitro* of single-stranded DNA molecules that fold into specific ligand-binding structures. *Nature*, **355**, 850–852.
6. Hermann,T. and Patel,D.J. (2000) Adaptive recognition by nucleic acid aptamers. *Science*, **287**, 820–825.
7. Shi,H., Hoffman,B.E. and Lis,J.T. (1999) RNA aptamers as effective protein antagonists in a multicellular organism. *Proc. Natl Acad. Sci. USA*, **96**, 10033–10038.
8. Thomas,M., Chedin,S., Carles,C., Riva,M., Famulok,M. and Sentenac,A. (1997) Selective targeting and inhibition of yeast RNA polymerase II by RNA aptamers. *J. Biol. Chem*., **272**, 27980–27986.
9. Werstuck,G. and Green,M.R. (1998) Controlling gene expression in living cells through small molecule–RNA interactions. *Science*, **282**, 296–298.
10. Martell,R.E., Nevins,J.R. and Sullenger,B.A. (2002) Optimizing aptamer activity for gene therapy applications using expression cassette SELEX. *Mol. Ther*., **6**, 30–34.
11. Sullenger,B.A., Gallardo,H.F., Ungers,G.E. and Gilboa,E. (1990) Overexpression of TAR sequences renders cells resistant to human immunodeficiency virus replication. *Cell*, **63**, 601–608.
12. Blind,M., Kolanus,W. and Famulok,M. (1999) Cytoplasmic RNA modulators of an inside-out signal-transduction cascade. *Proc. Natl Acad. Sci. USA*, **96**, 3606–3610.
13. Grad,J.M., Zeng,X.R. and Boise,L.H. (2000) Regulation of Bcl-xL: a little bit of this and a little bit of STAT. *Curr. Opin. Oncol*., **12**, 543–549.
14. Watanabe,M., Dewan,M.Z., Okamura,T., Sasaki,M., Itoh,K., Higashihara,M., Mizoguchi,H., Honda,M., Sata,T., Watanabe,T. *et al.* (2005) A novel NF-kappaB inhibitor DHMEQ selectively targets constitutive NF-kappaB activity and induces apoptosis of multiple myeloma cells *in vitro* and *in vivo*. *Int. J. Cancer*, **114**, 32–38.
15. Lebruska,L.L. and Maher,L.J.,III (1999) Selection and characterization of an RNA decoy for transcription factor NF-kappa B. *Biochemistry*, **38**, 3168–3174.
16. Cassiday,L.A. and Maher,L.J.,III (2003) Yeast genetic selections to optimize RNA decoys for transcription factor NF-kappa B.. *Proc. Natl Acad. Sci. USA*, **100**, 3930–3935.
17. Mi,J., Zhang,X., Giangrande,P.H., McNamaraII,J.O., Nimjee,S.M., Sarraf-Yazdi,S., Sullenger,B.A. and Clary,B.M. (2005) Targeted inhibition of αVβ3 integrin with an RNA aptamer impairs endothelial cell growth and survival. *Biochem. Biophys. Res. Commun*., **338**, 956–963.
18. Zhang,X., Kon,T., Wang,H., Li,F., Huang,Q., Rabbani,Z.N., Kirkpatrick,J.P., Vujaskovic,Z., Dewhirst,M.W. and Li,C.Y. (2004) Enhancement of hypoxia-induced tumor cell death *in vitro* and radiation therapy *in vivo* by use of small interfering RNA targeted t hypoxia-inducible factor-1 alpha. *Cancer Res*., **64**, 8139–8142.
19. Slebos,R.J. and Taylor,J.A. (2001) A novel host cell reactivation assay to assess homologous recombination capacity in human cancer cell lines. *Biochem. Biophys. Res. Commun*., **281**, 212–219.
20. Myslinski,E., Ame,J.C., Krol,A. and Carbon,P. (2001) An unusually compact external promoter for RNA polymerase III transcription of the human H1RNA gene. *Nucleic Acids Res*., **29**, 2502–2509.
21. Rusconi,C.P., Roberts,J.D., Pitoc,G.A., Nimjee,S.M., White,R.R., Quick,G.,Jr, Scardino,E., Fay,W.P. and Sullenger,B.A. (2004) Antidote-mediated control of an anticoagulant aptamer *in vivo*. *Nat. Biotechnol*., **22**, 1423–1428.
22. Cheng,Q., Lee,H.H., Li,Y., Parks,T.P. and Cheng,G. (2000) Upregulation of Bcl-x and Bfl-1 as a potential mechanism of chemoresistance, which can be overcome by NF-kappaB inhibition. *Oncogene*, **19**, 4936–4940.
23. King,D.J., Bassett,S.E., Li,X., Fennewald,S.A., Herzog,N.K., Luxon,B.A., Shope,R. and Gorenstein,D.G. (2002) Combinatorial selection and binding of phosphorothioate aptamers targeting human NF-kappa B RelA (p65) and p50. *Biochemistry*, **41**, 9696–9706.
24. Arenzana-Seisdedos,F., Turpin,P., Rodriguez,M., Thomas,D., Hay,R.T., Virelizier,J.L. and Dargemont,C. (1997) Nuclear localization of I kappa B alpha promotes active transport of NF-kappa B from the nucleus to the cytoplasm. *J. Cell Sci*., **110**, 369–378.
25. Bharti,A.C. and Aggarwal,B.B. (2002) Nuclear factor-kappa B and cancer: its role in prevention and therapy. *Biochem. Pharmacol*., **64**, 883–888.
26. Greten,F.R. and Karin,M. (2004) The IKK/NF-kappaB activation pathway-a target for prevention and treatment of cancer. *Cancer Lett*., **206**, 193–199.
27. Matsukura,S., Jones,P.A. and Takai,D. (2003) Establishment of conditional vectors for hairpin siRNA knockdowns. *Nucleic Acids Res*., **31**, e77.
28. Ohkawa,J. and Taira,K. (2000) Control of the functional activity of an antisense RNA by a tetracycline-responsive derivative of the human U6 snRNA promoter. *Hum. Gene Ther*., **11**, 577–585.